

Double Universality of a Quantum Phase Transition in Spinor Condensates: Modification of the Kibble-Žurek Mechanism by a Conservation Law

Tomasz Świsłocki,¹ Emilia Witkowska,¹ Jacek Dziarmaga,² and Michał Matuszewski¹

¹*Instytut Fizyki PAN, Aleja Lotników 32/46, 02-668 Warsaw, Poland*

²*Instytut Fizyki Uniwersytetu Jagiellońskiego, ul. Reymonta 4, 30-059 Kraków, Poland*

(Received 24 August 2012; published 24 January 2013)

We consider a phase transition from an antiferromagnetic to a phase separated ground state in a spin-1 Bose-Einstein condensate of ultracold atoms. We demonstrate the occurrence of two scaling laws, for the number of spin domain seeds just after the phase transition, and for the number of spin domains in the final, stable configuration. Only the first scaling can be explained by the standard Kibble-Žurek mechanism. We explain the occurrence of two scaling laws by a model including postselection of spin domains due to the conservation of condensate magnetization.

DOI: 10.1103/PhysRevLett.110.045303

PACS numbers: 67.85.De, 03.75.Mn, 05.30.Rt, 67.85.Fg

The idea of a nonequilibrium phase transition has been attracting a great deal of attention in many branches of physics. The number of physical models where it has been considered or observed is steadily growing, now including not only the dynamics of the early Universe [1] and superfluid helium [2,3], but also superconductors [4], cold atomic gases [5], and other systems [6]. The most notable outcome of such a phase transition is the possible creation of defects, such as monopoles, strings, vortices or solitons [1,2,7] after crossing the critical point at a finite rate. The Kibble-Žurek mechanism (KZM) is a theory that allows us to predict the density of created defects from the knowledge of the correlation length ξ at the instant when the system goes out of equilibrium [2]. The resulting scaling displays universal behavior and is dependent only on the critical exponents of the system ν and z .

Quantum phase transition, in contrast to a classical (thermodynamic) one, occurs when varying a physical parameter leads to a change of the nature of the ground state [8]. Recently, a few theoretical works demonstrated that the KZM can be successfully applied to describe quantum phase transitions in several models [9–13], see Ref. [14] for reviews. Among these, Bose-Einstein condensates of ultracold atoms offer realistic models of highly controllable and tunable systems [12,13]. In Ref. [13], the miscibility-immiscibility phase transition leading to the formation of stable, stationary domains was proposed as an ideal candidate to observe KZM scaling in a quantum phase transition.

In this Letter, we investigate the critical scaling of the number of defects created during the transition to the phase separated state of an antiferromagnetic spin-1 condensate [15–17]. The introduction of a weak magnetic field can lead in these systems to the transition from an antiferromagnetic ground state to a state where domains of atoms with different spin projections separate [16]. In contrast to the transition considered in Ref. [13], our scheme does not require the use of microwave coupling field or Feshbach

resonances, which makes the experiment simpler and more stable against inelastic losses.

By employing numerical simulations within the truncated Wigner approximation, we make a quite unexpected observation. While the number of spin domain seeds just after the phase transition closely follows the predictions of the KZM, the number of spin domains in the final, stabilized state is given by a scaling law with a different exponent. We explain this double universality and predict the value of the second exponent using a model of system dynamics including later stages of evolution, no longer described by the standard KZM. We show that when the nonlinear processes set in, an effective postselection of spin domains takes place, after which only a part of them can survive due to the conservation of the condensate magnetization.

We consider a dilute antiferromagnetic spin-1 BEC in a homogeneous magnetic field pointing along the z axis. We start with the Hamiltonian $H = H_0 + H_A$, where the symmetric (spin independent) part is

$$H_0 = \sum_{j=-,0,+} \int dx \psi_j^\dagger \left(-\frac{\hbar^2}{2m} \nabla^2 + \frac{c_0}{2} n + V(x) \right) \psi_j,$$

where the subscripts $j = -, 0, +$ denote sublevels with magnetic quantum numbers along the magnetic field axis $m_j = -1, 0, +1$, m is the atomic mass, $n = \sum_j n_j = \sum_j \psi_j^\dagger \psi_j$ is the total atom density, and $V(x)$ is the external potential. Here we restricted the model to one dimension, with the other degrees of freedom confined by a strong transverse potential with frequency ω_\perp . The spin-dependent part can be written as

$$H_A = \int dx \left(\sum_j E_j n_j + \frac{c_2}{2} : \mathbf{F}^2 : \right),$$

where E_j are the Zeeman energy levels and the spin density is $\mathbf{F} = (\psi^\dagger F_x \psi, \psi^\dagger F_y \psi, \psi^\dagger F_z \psi)$ where $F_{x,y,z}$ are the spin-1 matrices and $\psi = (\psi_+, \psi_0, \psi_-)$. The

spin-independent and spin-dependent interaction coefficients are given by $c_0 = 2\hbar\omega_\perp(2a_2 + a_0)/3 > 0$ and $c_2 = 2\hbar\omega_\perp(a_2 - a_0)/3 > 0$, where a_S is the s -wave scattering length for colliding atoms with total spin S . The total number of atoms $N = \int n dx$ and magnetization $M = \int (n_+ - n_-) dx$ are conserved. In reality, there are processes that can lead to a change of both N and M , but they are relatively weak in ^{23}Na condensates, and we can neglect them on the length scales considered below.

The linear part of the Zeeman effect induces a homogeneous rotation of the spin vector around the direction of the magnetic field. Since the Hamiltonian is invariant with respect to such spin rotations, we consider only the effects of the quadratic Zeeman shift [16]. For a sufficiently weak magnetic field we can approximate it by a positive energy shift of the $m_f = \pm 1$ sublevels $\delta = (E_+ + E_- - 2E_0)/2 \approx B^2 A$, where B is the magnetic field strength and $A = (g_I + g_J)^2 \mu_B^2 / 16 E_{\text{HFS}}$, g_I and g_J are the gyromagnetic ratios of electron and nucleus, μ_B is the Bohr magneton, and E_{HFS} is the hyperfine energy splitting at zero magnetic field [16].

The ground state phase diagram, shown in Fig. 1(a), contains three phases divided by two critical points at $B_1 = B_0 M / \sqrt{2} N$ and $B_2 = B_0 / \sqrt{2}$, where $B_0 = \sqrt{c_2 n / A}$ and n is the total density. The ground state can be (i) antiferromagnetic (2C) with $\psi = (\psi_+, 0, \psi_-)$ for $B < B_1$, (ii) phase separated into two domains of the 2C and $\psi = (0, \psi_0, 0)$ -type (ρ_0) for $B \in (B_1, B_2)$, or (iii) phase separated into two domains of the ρ_0 and $\psi = (\psi_+, 0, 0)$ -type (ρ_+) for $B > B_2$ [16]. Note that the phase diagram is different in the special cases $M = 0, \pm N$, which we disregard in the current Letter.

For simplicity, we consider a system in the ring-shaped quasi-1D geometry with periodic boundary conditions at $\pm L/2$ and $V(x) = 0$. The magnetic field is initially switched off, and the atoms are prepared in the antiferromagnetic (2C) ground state with magnetization fixed to $M = N/2$ (without loss of generality). To investigate the KZM we increase B linearly during the time τ_Q to drive the system through one or two phase transitions into a phase separated state. Due to the finite quench time, the system ends up in a state with multiple spin domains.

The Kibble-Zurek theory is a powerful tool that allows us to predict the density of topological defects resulting from a nonequilibrium phase transition without solving the full dynamical equations. The concept relies on the fact

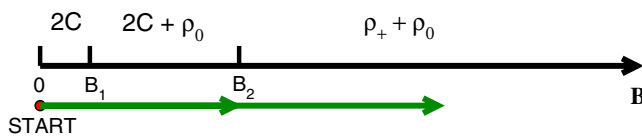


FIG. 1 (color online). Ground state phase diagram of an antiferromagnetic condensate for magnetization $M = N/2$. We increase B linearly during the time τ_Q to drive the system through one or two phase transitions into a phase separated state.

that the system does not follow the ground state exactly in the vicinity of the critical point due to the divergence of the relaxation time. The dynamics of the system cease to be adiabatic at $t \approx -\hat{t}$ (here we choose $t = 0$ in the first critical point), when the relaxation time becomes comparable to the inverse quench rate

$$\hat{\tau}_{\text{rel}} \approx |\hat{\varepsilon}/\dot{\hat{\varepsilon}}|, \quad (1)$$

where $\varepsilon(t) = B - B_1 \sim t/\tau_Q$ is the distance of the system from the critical point. At this moment, the fluctuations approximately freeze, until the relaxation time becomes short enough again. After crossing the critical point, distant parts of the system choose to break the symmetry in different ways, which leads to the appearance of multiple defects in the form of domain walls between domains of 2C and ρ_0 phases. The average number of domains is related to the correlation length $\hat{\xi}$ at the freeze-out time $\hat{t} \sim \tau_Q^{z\nu/(1+z\nu)}$ [2,14]

$$N_d = L/\hat{\xi} \sim \tau_Q^{-\nu/(1+z\nu)}, \quad (2)$$

where z and ν are the critical exponents determined by the scaling of the relaxation time $\tau_{\text{rel}} \sim |\varepsilon|^{-z\nu}$ and excitation spectrum $\omega \sim |k|^z$, with $z = 1$ in the superfluid.

We test the above prediction in numerical simulations within the truncated Wigner approximation, with $N = 10^6$ and parameters close to that of previous experiments in ^{23}Na [15]. Additionally, we consider a “cleaner” case with transition through the first critical point only and $N = 20 \times 10^6$ in order to minimize merging of domains. Typical results of a single run, which can be interpreted as a single realization, are shown in Fig. 2. We can clearly see the process of domain formation after the first phase transition at t_1 . However, there is always some number of domain seeds that disappear instead of evolving into full domains, see Fig. 2(f).

The above dynamics have a striking effect on the number of defects that are created in the system. In Fig. 3 we show the average number of defects in the function of the quench time τ_Q for the “cleaner” case of a large number of atoms, as in Fig. 2(e). The critical exponents, calculated from the Bogoliubov excitation spectrum of the relevant gapped mode with $\Delta_B = c_2 n \sqrt{(\delta/c_2 n - 1)^2 - (1 - M^2/N^2)}$ are identical as in the case of a ferromagnetic [12] or two-component [13] condensate, $z = 1$ and $\nu = 1/2$. According to Eq. (2), we could expect the scaling $N_d \sim \tau_Q^{-1/3}$. However, the number of domains in the final, stabilized state scales approximately as $N_d \sim \tau_Q^{-2/3}$ in a wide range of τ_Q , as depicted with the dashed line. Nevertheless, if we count the number of domain seeds [18] just after the first phase transition, we do recover the $N_s \sim \tau_Q^{-1/3}$ dependence (inset).

We explain this puzzling appearance of two different scaling exponents with a model that includes several

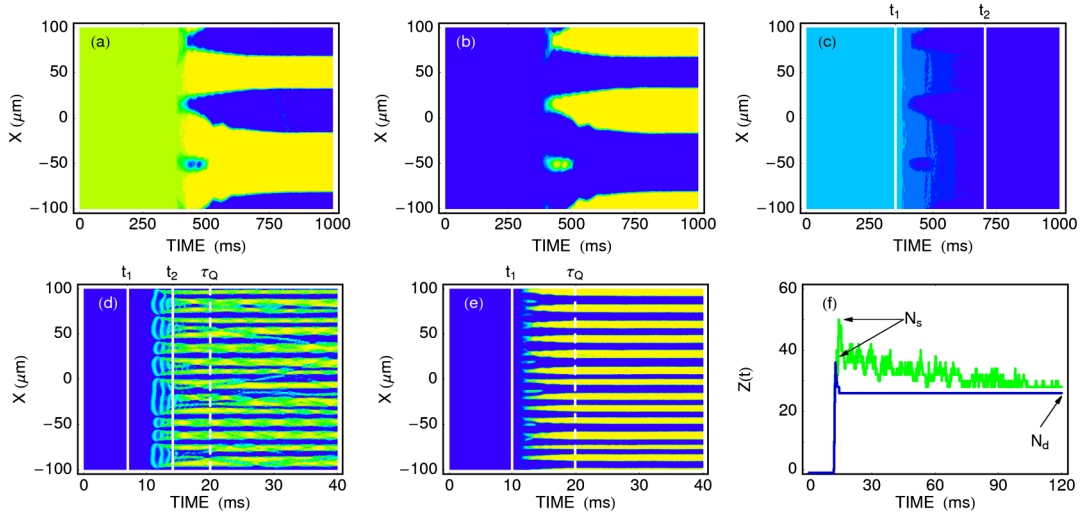


FIG. 2 (color online). Spin domain formation dynamics in a ring-shaped 1D geometry with ring length $L = 200 \mu\text{m}$ and $\omega_{\perp} = 2\pi \times 1000 \text{ Hz}$. The top row shows densities (lighter is higher) of ψ_+ (a), ψ_0 (b), and ψ_- (c) for $N = 10^6$ atoms, quench time $\tau_Q = 1 \text{ s}$, and final magnetic field strength $B/B_0 = 1$. The vertical lines at t_1 and t_2 correspond to the two phase transitions from Fig. 1(a). In (d) and (e), ψ_0 densities for faster quenches with $\tau_Q = 20 \text{ ms}$ are shown. The number of atoms in (e) is increased to $N = 20 \times 10^6$ and final magnetic field is $(B/B_0)^2 = 0.49$ to show a cleaner process with a single phase transition and without interaction of fully formed domains. Frame (f) shows the function $Z(t)$, defined by Ref. [18], which allows us to determine the number of domain seeds N_s and the final number of spin domains N_d . The light line corresponds to (d), while the dark line corresponds to (e).

phases of the domain formation process, see Fig. 4. The 2C state becomes unstable shortly after crossing the first critical point at $B = B_1$. Initially, the system follows the standard Kibble-Zurek scenario, as the spin fluctuations start to grow exponentially at the freeze-out time $\hat{t} \sim \tau_Q^{1/3}$, see Fig. 4(a). We now count the number of small spin domain

seeds [18], which scales in the same way as the number of defects in the Kibble-Zurek theory, $N_s \sim \tau_Q^{-1/3}$. At this point the KZM is completed, but it turns out to be just a prelude to the ultimate postselection mechanism that sets the final density of domains N_d .

As the fluctuations grow, they leave the linearized Bogoliubov regime and approach the instantaneous ground state, which is the phase separated $2C + \rho_0$ state [16]. The equilibrium between the 2C and ρ_0 phases requires equal energy density (pressure) in both phases. In the limit $c_2 \ll c_0$, the atom density n is the same in both phases, and one obtains the simple condition $\frac{B}{B_0} = \frac{M_{2C}}{\sqrt{2}N_{2C}}$, where $M_{2C} = M$ is the total magnetization of the 2C phase, and N_{2C} the number of atoms in this phase. Since the total magnetization in the system $M = \int(n_+ - n_-)dx$ is a conserved quantity, the above impose the condition on the fraction of total volume occupied by the ρ_0 phase, $x_0 = 1 - N_{2C}/N$,

$$x_0 = 1 - \frac{M}{\sqrt{2}N} \frac{B_0}{B} = 1 - \frac{B_1}{B}. \quad (3)$$

Note that soon after the phase transition, when $B \approx B_1$, it is small and so is the volume occupied by the ρ_0 phase.

The volume occupied by the fluctuations that choose to approach the ρ_0 phase is limited by the constraint of Eq. (3). Therefore, as the fluctuations grow in magnitude they are forced to concentrate into small ‘‘bubbles,’’ see Fig. 4(b). In the process some of the bubbles must disappear because the minimal width of a ρ_0 domain is set by several spin healing lengths $\xi_s = (B_0/B)^2 \hbar / \sqrt{2mc_2 n}$, see

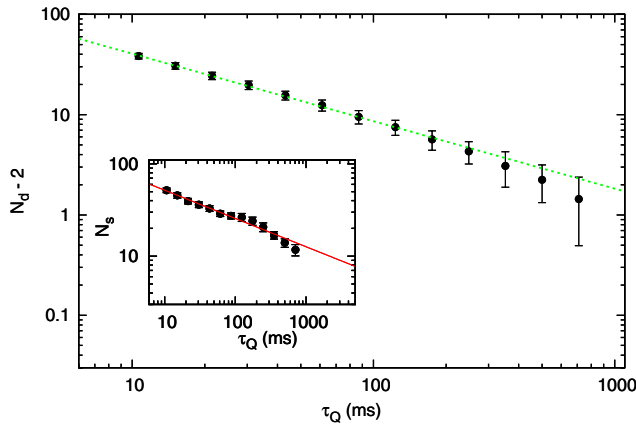


FIG. 3 (color online). Averaged number of spin domains after the quench as a function of the quench time for $N = 20 \times 10^6$. The scale is logarithmic on both axes and N_d is decreased by two to account for the ground state phase separation into two domains. The points are results of truncated Wigner simulations averaged over 100 runs. The dashed line is the fit to the power law with scaling exponent $n_d = -0.67 \pm 0.01$. The inset shows the number of spin domain seeds counted just after the phase transition. The scaling exponent here is found to be $n_s = -0.32 \pm 0.01$.

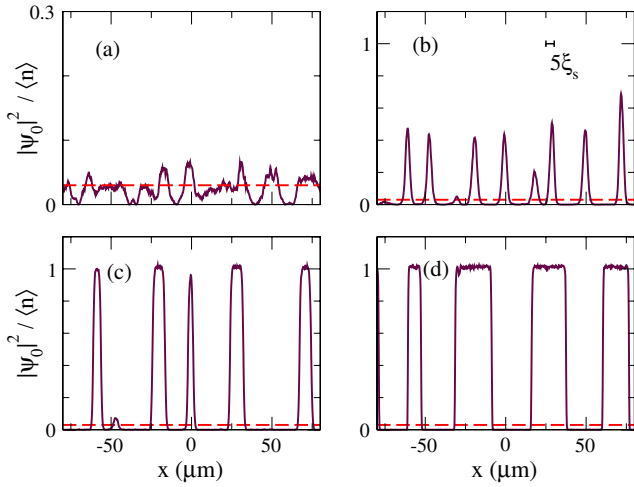


FIG. 4 (color online). Profiles of the density $|\psi_0|^2$ for $\tau_Q = 100$ ms, showing four consecutive phases of the domain formation process after crossing the first critical point. (a) At $t = 53.5$ ms the small spin fluctuations begin to grow exponentially, forming spin domain seeds. (b) At $t = 56$ ms the seeds transform into narrow (several ξ_s) bubbles of ψ_0 . (c) At $t = 65$ ms, as the bubbles mature, the postselection eliminates some of them to keep the magnetization conserved. (d) At $t = 100$ ms, the domains have gradually increased in size and occupy half of the available area at $B = 2B_1$. The dashed horizontal line corresponds to α used to calculate $Z(t)$ [18]. The formation of the stable ρ_0 bubbles in the stages (a), (b), and (c) takes place in the narrow time interval $t = 53.5, \dots, 65$ around \hat{t} . The magnetic field \hat{B} within this relatively short time span satisfies $\hat{B} - B_1 \sim \hat{t}/\tau_Q \sim \tau_Q^{-2/3}$.

Fig. 4(c). This healing length is finite near the phase transition and we have confirmed numerically that the minimal bubble size is independent of τ_Q .

For slow quenches $\hat{t} \sim \tau_Q^{1/3}$ is the longest relevant time scale near the phase transition and, therefore, for the sake of the scaling argument it is safe to say that the bubbles form near \hat{t} . This time corresponds to \hat{B} , such that $\hat{B} - B_1 \sim \hat{t}/\tau_Q \sim \tau_Q^{-2/3}$, which is close to the critical point. Consequently, the fraction $\hat{x}_0 = 1 - B_1/\hat{B}$ of the volume occupied by the bubbles at \hat{B} is small and scales as $\hat{x}_0 \sim \tau_Q^{-2/3}$. The number of ρ_0 bubbles is thus $N_d \sim \hat{x}_0/\xi_s \sim \tau_Q^{-2/3}$. This is also the final postselected density of domain walls compatible with the conserved magnetization.

Once the domains are stabilized they gradually grow in size with $x_0 = 1 - B_1/B$ as the magnetic field is further increased, see Fig. 4(d). In this last long stage of the evolution the domains are stable except for possible phase ordering kinetics [19]. This is a slow process where fluctuations eventually merge some domains slowly reducing the domain number N_d . The fluctuations are stronger for a lower number of atoms. In Fig. 5, we plot the number of created defects for a lower (realistic) number of atoms

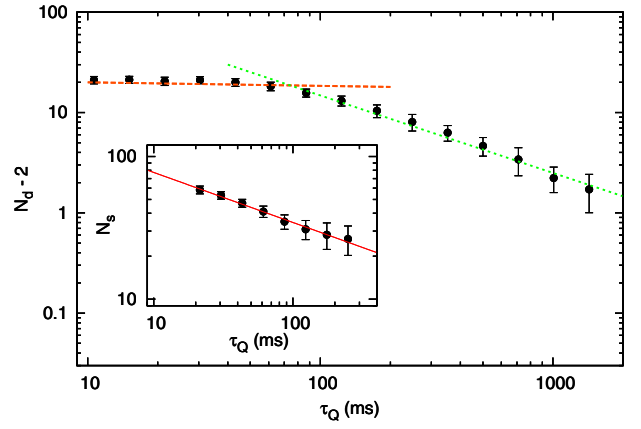


FIG. 5 (color online). Similar as in Fig. 3, but for a realistic case of $N = 10^6$. Here, the horizontal dashed line shows the saturation of the number of domains due to the finite spin healing length. The scaling exponents in this case are $n_d = -0.71 \pm 0.03$ and $n_s = -0.35 \pm 0.01$.

$N = 10^6$ [15]. The interactions are weaker in this case, which results in a longer spin healing length ξ_s , which sets the smallest possible domain size and is responsible for the saturation of the number of domains for small τ_Q . Nevertheless, we can still clearly see the two different scaling laws for N_s and N_d in a wide range of quench times τ_Q . Here, the scaling exponents appear to be slightly smaller than in the previous, “cleaner” case. Since the final state with multiple domains is not a true ground state, but a metastable state [15], we attribute this difference to the phase ordering kinetics, which effectively decrease the scaling exponents [19]. However, the slow phase ordering taking place on a time scale much longer than \hat{t} should be distinguished from the postselection that happens near the same \hat{t} as the KZM.

In conclusion, we investigated a nonequilibrium phase transition in a relatively simple and stable experiment in an antiferromagnetic Bose-Einstein condensate. We demonstrated the occurrence of two scaling laws describing the number of spin domain seeds and the final number of spin domains. The occurrence of two scaling laws was explained in a model of system dynamics including an effective postselection of spin domains due to the conservation of magnetization. The postselection transforming the scaling law is a general mechanism that should be effective whenever the standard Kibble-Zurek mechanism is not compatible with an additional conservation law.

We thank Wojciech Żurek for reading the manuscript and useful comments. This work was supported by the Polish Ministry of Science and Education Grants No. N N202 128539 and No. IP 2011 034571, the National Science Center Grants No. DEC-2011/01/B/ST3/00512 and No. DEC-2011/03/D/ST2/01938, and by the Foundation for Polish Science through the “Homing Plus” program.

- [1] T. W. B. Kibble, *J. Phys. A* **9**, 1387 (1976); *Phys. Rep.* **67**, 183 (1980).
- [2] W. H. Żurek, *Nature (London)* **317**, 505 (1985); *Acta Phys. Pol. B* **24**, 1301 (1993); *Phys. Rep.* **276**, 177 (1996).
- [3] C. Bauerle, Yu. M. Bunkov, S. N. Fisher, H. Godfrin, and G. R. Pickett, *Nature (London)* **382**, 332 (1996); V. M. H. Ruutu, V. B. Eltsov, A. J. Gill, T. W. B. Kibble, M. Krusius, Yu. G. Makhlin, B. Plaçais, G. E. Volovik, and W. Xu, *ibid.* **382**, 334 (1996).
- [4] A. Maniv, E. Polturak, and G. Koren, *Phys. Rev. Lett.* **91**, 197001 (2003); R. Monaco, J. Mygind, M. Aaroe, R. Rivers, and V. Koshelets, *ibid.* **96**, 180604 (2006).
- [5] L. E. Sadler, J. M. Higbie, S. R. Leslie, M. Vengalattore, and D. M. Stamper-Kurn, *Nature (London)* **443**, 312 (2006); M. Lewenstein, A. Sanpera, V. Ahufinger, B. Damski, A. Sen(De), and U. Sen, *Adv. Phys.* **56**, 243 (2007); C. N. Weiler, T. W. Neely, D. R. Scherer, A. S. Bradley, M. J. Davis, and B. P. Anderson, *Nature (London)* **455**, 948 (2008); E. Witkowska, P. Deuar, M. Gajda, and K. Rzażewski, *Phys. Rev. Lett.* **106**, 135301 (2011).
- [6] I. Chuang, R. Durrer, N. Turok, and B. Yurke, *Science* **251**, 1336 (1991).
- [7] B. Damski and W. H. Żurek, *Phys. Rev. Lett.* **104**, 160404 (2010).
- [8] S. Sachdev, *Quantum Phase Transitions* (Cambridge University Press, Cambridge, England, 2001).
- [9] J. Dziarmaga, *Phys. Rev. Lett.* **95**, 245701 (2005).
- [10] W. H. Żurek, U. Dorner, and P. Zoller, *Phys. Rev. Lett.* **95**, 105701 (2005).
- [11] B. Damski, *Phys. Rev. Lett.* **95**, 035701 (2005).
- [12] A. Lamacraft, *Phys. Rev. Lett.* **98**, 160404 (2007); B. Damski and W. H. Żurek, *Phys. Rev. Lett.* **99**, 130402 (2007); H. Saito, Y. Kawaguchi, and M. Ueda, *Phys. Rev. A* **76**, 043613 (2007).
- [13] J. Sabbatini, W. H. Żurek, and M. J. Davis, *Phys. Rev. Lett.* **107**, 230402 (2011).
- [14] J. Dziarmaga, *Adv. Phys.* **59**, 1063 (2010); A. Polkovnikov, K. Sengupta, A. Silva, and M. Vengalattore, *Rev. Mod. Phys.* **83**, 863 (2011).
- [15] J. Stenger, S. Inouye, D. M. Stamper-Kurn, H.-J. Miesner, A. P. Chikkatur, and W. Ketterle, *Nature (London)* **396**, 345 (1998); H.-J. Miesner, D. M. Stamper-Kurn, J. Stenger, S. Inouye, A. P. Chikkatur, and W. Ketterle, *Phys. Rev. Lett.* **82**, 2228 (1999).
- [16] M. Matuszewski, T. J. Alexander, and Y. S. Kivshar, *Phys. Rev. A* **80**, 023602 (2009).
- [17] M. Matuszewski, T. J. Alexander, and Y. S. Kivshar, *Phys. Rev. A* **78**, 023632 (2008); M. Matuszewski, *Phys. Rev. Lett.* **105**, 020405 (2010); *Phys. Rev. A* **82**, 053630 (2010).
- [18] $Z(t)$ is the number of zero crossings of the function $f(x) = n_0(x) - \alpha N/L$ at a given time t , where $\alpha = 0.03$. Then, the number of spin domain seeds N_s corresponds to the maximum value of $Z(t)$ over the entire simulation time. We checked that this method is accurate and weakly dependent on the choice of α .
- [19] A. J. Bray, *Adv. Phys.* **43**, 357 (1994).